

## ORIGINAL ARTICLE

# Biological effectiveness and relative biological effectiveness of ion beams for in-vitro cell irradiation

Heng Li 

Department of Radiation Oncology and Molecular Radiation Sciences, Johns Hopkins University, Baltimore, MD, USA

**Correspondence**

Heng Li, Department of Radiation Oncology and Molecular Radiation Sciences, Johns Hopkins University, 401 N. Broadway, Baltimore, MD 21287, USA.  
Email: [hengli@jhu.edu](mailto:hengli@jhu.edu)

**Abstract**

Biological effectiveness and relative biological effectiveness are critical for proton and ion beam radiotherapy. However, the relationship between the two quantities and physical character of ion beams is not well established. By analyzing 1188 sets of in-vitro cell irradiation experiments using ion beams ranging from protons to  $^{238}\text{U}$ , compiled by the Particle Irradiation Data Ensemble (PIDE) project, the biological effectiveness of the ion beams, with cell survival fractionation (SF) as the endpoint, was found to be dependent on the fluence and linear energy transfer (LET) of the ion beam. Consequently, the relative biological effectiveness of the ion beam to photon beam was also established as a function of LET. A common form of relationship among SF, fluence, and LET was found to be valid for all ion beam experiments. The close form relationship could be used for proton and ion beam radiotherapy applications.

**KEYWORDS**

biological effectiveness, in-vitro radiation, ion beam, modeling, radiation

## 1 | INTRODUCTION

Biological effects of ionization radiation include cell killing, carcinogenesis, and mutation.<sup>1</sup> The principal target of ionization radiation for these biological effects is DNA.<sup>2</sup> Extensive in-vivo experiments have been performed to investigate the relationship between ionizing radiation and cell death, among other biological endpoints.<sup>3-7</sup>

The absorbed dose of ionizing radiation has been used to relate the imparted radiation energy to biological effects, specifically for in-vitro cell experiments, cell death, and survival fractionations. The widely accepted linear quadratic (LQ) model establishes the relationship between absorbed dose and cell survival fractionation and has been extensively used to analyze and predict ionizing radiation response both in vitro and in vivo.<sup>8</sup> Ions, or charged particles, could have physical and radiobiological advantages over photon irradiation

for radiation therapy.<sup>9</sup> The radiobiological advantage of ion beam irradiation manifests in the form of more effective cell killing with the same absorbed dose for in-vitro cell irradiation experiments.<sup>10</sup> Different ion beams and beams with the same ion but with different kinetic energies (and, thus, different linear energy transfer, LET) have different biological effectiveness, which is not reflected in the dose-survival model; that is, the same absorbed dose delivered by different ion beams or the same ion beam with different LET would yield different survival fractionation for the same cell line.<sup>11</sup> The difference in biological effect between low and high LET radiation could affect human exploration of outer space as the space radiation has high LET components that need to be accounted for.<sup>12</sup>

Because of the observed difference of dose needed to achieve the same biological endpoint for ion beams, relative biological effectiveness (RBE), defined as the ratio of the doses required by

**Abbreviations:** DSB, double strand break; LET, linear energy transfer; LQ, linear quadratic; PIDE, Particle Irradiation Data Ensemble; RBE, relative biological effectiveness; SF, survival fractionation.

This is an open access article under the terms of the [Creative Commons Attribution-NonCommercial-NoDerivs](https://creativecommons.org/licenses/by-nc-nd/4.0/) License, which permits use and distribution in any medium, provided the original work is properly cited, the use is non-commercial and no modifications or adaptations are made.

© 2022 The Author. *Cancer Science* published by John Wiley & Sons Australia, Ltd on behalf of Japanese Cancer Association.

two different types of radiation beams to cause the same level of biological effect, was introduced to account for the difference.<sup>13-15</sup> Although considerable research, including both experiment and modeling efforts, has been undertaken, the relationship between the (relative) biological effectiveness of ion beam and dose, or other descriptors of the ion beam characteristic, remains unclear.<sup>16</sup>

Defined as the amount of energy absorbed by matter per unit mass,<sup>17</sup> the absorbed dose could be represented as the product of fluence and LET.<sup>18</sup> By definition, LET is the energy loss per unit length and could be considered a measurement of the density of ionization events around ion tracks, whereas fluence represents the number of ion tracks per unit area. Ionization events, induced by ionizing radiation, cause DNA damage, including double strand breaks (DSB) and cluster damage, which in turn leads to cell death. In this context, it became clear that, unlike photon irradiation, for which the spatial distribution of ionization events could be in general considered uniform, the spatial distribution of the energy deposition and ionization events plays an essential role in the biological effectiveness of the ion beam. This is because more ionization events near DNA in the cell nucleus, in general, would be more damaging to the cell. Therefore, dose is not adequate for use as the sole parameter to quantify the biological effects of ion beams because of the lack of spatial information.

Models have been proposed to describe the relative biological effects of ion beams. The most notable models are the local effect model (LEM),<sup>19-22</sup> the (modified) microdosimetric kinetic model (MKM),<sup>23-25</sup> and the repair-misrepair-fixation (RMF) model.<sup>26,27</sup> In general, to establish the relationship between the reference photon irradiation and the ion beam irradiation, specific and unvalidated assumptions were made for each of these models. For example, Scholz and Kraft stated in a commentary that “the fundamental assumption of the LEM is that the local biological effect is determined by the local dose, but is independent of the particular radiation type leading to a given local dose” (Radiation Research 161, Page 612).<sup>28</sup> The direct comparison among these models for the same beam condition found large discrepancies in their predictions, indicating that the underlying assumptions in these models might not be valid.<sup>29</sup>

In this study, it was hypothesized that as opposed to dose and RBE, a different function of fluence and LET could describe the biological effectiveness of ion beam radiation. The description of biological effectiveness could subsequently be used for comparison with the reference photon irradiation to determine RBE, thereby avoid making any assumptions on the relationship between the photon and ion beam irradiation. By analyzing 1118 sets of in-vitro cell experiments with ion beams, compiled by the Particle Irradiation Data Ensemble (PIDE) project,<sup>16</sup> a common form was established to describe the survival fractionation of all cell experiments.

## 2 | MATERIALS AND METHODS

It has been widely accepted that the post-irradiation cell survival fractionation (SF) follows a linear quadratic relationship (LQ model) with an absorbed dose for photon and ion beam radiation.<sup>8</sup>

$$SF = e^{-(\alpha D + \beta D^2)}, \quad (1)$$

where parameters  $\alpha$  and  $\beta$  are usually determined by experiments and vary with cell type and type of radiation.  $D$  is the absorbed dose:

$$D(\text{Gy}) = \frac{dE}{dm} = \frac{\Phi L_{\infty}}{\rho} = 1.602 \times 10^{-1} \times \Phi (1/\mu\text{m}^2) \times L_{\infty}(\text{keV}/\mu\text{m}) \times 1/\rho(\text{cm}^3/\text{g}) \quad (2)$$

Absorbed dose is defined as the amount of energy imparted to matter by ionizing radiation per unit mass of the matter and could be represented as a product of  $\Phi$  and  $L_{\infty}$ . In this equation,  $\Phi$  is the fluence of the ion beam,  $\rho$  is the density of the medium, and  $L_{\infty}$  is the unrestricted LET, defined as the energy loss per unit distance, and is the same as stopping power.<sup>18</sup>

As mentioned above, the dose could be represented by the product of fluence and LET. Although the effect of LET in ion beam radiation has been extensively studied, the role of fluence has not been investigated. It is well established that the RBE of ion beam irradiation rises with LET up to a certain point and then declines. In other words, using the same ion type beam with varying LETs, the dose required to achieve the same biological endpoint declines with LET up to a certain point; then the required dose to reach the said biological endpoint increases.<sup>30</sup> The so called “overkill” effect has different “turning point” for different ions but is usually considered to be approximately 100 to 200 keV/ $\mu\text{m}$ .<sup>31</sup> In this LET range, the average separation of ionization events introduced by a single ion is thought to coincide with the diameter of the DNA helix. Therefore, it is effective in introducing DNA DSB or clustered damage that leads to cell death. For ions with even higher LET, the denser ionization event may cause more localized damage but not result in more cell death.

The fluence-LET combination needed to achieve a specific SF could be found from the fluence-LET-SF surface. When plotted on a log-log scale, Equation (2) becomes

$$\log(\Phi) = \log(D) - \log(L_{\infty}). \quad (3)$$

However, it could be observed from the PIDE data that the fluence-LET on the iso-SF plane does not follow Equation (3). Instead, it follows a line with a different slope, as described by:

$$\log(\Phi) = \log(D_1) - c \log(L_{\infty}), \quad (4)$$

where  $c$  is the slope of the line, and  $D_1$  is the intersection of the line and LET of 1 keV/ $\mu\text{m}$ . The equation and the relationship among SF, LET, and fluence could then be written as:

$$SF = e^{-aD_1^b} \quad (5)$$

$$D_1 = \Phi L_{\infty}^c, \quad (6)$$

where parameters  $a$  and  $b$  vary with cell type and ion type;  $c$  varies with  $\Phi$ ,  $L_{\infty}$ , cell type, and ion type and is a bijective function of SF; and  $D_1$  is also a bijective function of SF. In this formalism,  $D_1$

TABLE 1 The number of experiments compiled in the PIDE project presented for a subset of ions and cell lines with more than 15 sets of experiments

	V79 asynchronous													Other cell lines
	Total	V79	cell phase	T1	HSG	NB1RGB	C3H10T1/2	CHO	B14FAF28	R-1	HF19	AG01522	SQ20B	
X-ray	261	49	37	6	1	5	17	6	1	1	5	6	4	160
1H	180	52	50				8				3	14	3	100
2H	17	10	4				5							2
3He	44	31	23		12		1							
4He	107	36	26	7			7				10	3		44
12C	385	70	61	22	21	24	2	14		11	4	3	11	203
20Ne	131	23	20	23	21	15	1	9		11		2		26
40Ar	57	21	17	11			1	1	6	6		1	1	9
Other ions	197	77	77	6		12	9	10	24	24	8	5		46
Ions total	1118	320	278	69	54	51	34	34	30	28	25	28	15	430

Note: 1H: hydrogen ion with a mass number of 1 (proton). Empty cells represent that no experiments were performed using the combination of ion and cell line.

numerically equals the dose required to achieve SF for a particular ion beam with LET of 1 keV/μm.

The following method was applied to the 1118 sets of experiments compiled by the PIDE project. PIDE collected LET,  $\alpha$ ,  $\beta$ , cell line, and ion type for in-vitro cell irradiation experiments with ion beams from 115 publications between 1965 and 2015. The complete list of these 115 publications as compiled by PIDE is shown in Appendix S1.

1. For each cell line, and
2. For each ion type, the sets of experiments performed with the given cell line and ion type were identified with LET,  $\alpha$ , and  $\beta$ .
3. For each set of experiments, a series of SF was chosen, and the corresponding dose  $D$  to achieve each of the SF was calculated by solving Equation (1) with known  $\alpha$ ,  $\beta$ .
4. Fluence  $\Phi$  was calculated with  $D$  and LET using Equation (2)
5. For each SF,  $D_1$  and  $c_L$  were determined with the linear fit for data points with LET  $\leq 150$  keV/μm
6. Separately, for each SF,  $D_1$  and  $c_H$  were determined with linear fit with all ion beam data with LET  $> 150$  keV/μm

With Equations (5) and (6), it is straightforward to calculate RBE for any ion type with given SF:

$$RBE_{\text{type}} = D_{\text{ref}} / D_{\text{type}} \quad (7)$$

Specifically, for in-vitro cell irradiation experiments, the RBE was evaluated with cell SF as the biological endpoint, where RBE is the ratio between doses required to achieve the same SF for photon (ref) and ion beam (type) radiation:

$$RBE_{\text{type}}(\text{SF}) = D_{\text{ref}}(\text{SF}) / D_{\text{type}}(\text{SF}) \quad (8)$$

$$RBE_{\text{type}}(\text{SF}) = \frac{D_{\text{ref}}(\text{SF})}{D_{\text{type}}(\text{SF})} = \frac{D_{\text{ref}}(\text{SF})}{\Phi(\text{SF})L_{\infty}} = \frac{D_{\text{ref}}(\text{SF})}{D_1(\text{SF})} (L_{\infty})^{c-1} \quad (9)$$

Since  $D_{\text{ref}}$ ,  $D_1$ , and  $c$  are all bijective functions of SF, LET becomes the only variable for RBE for any given SF, which is consistent with the previous "widespread assumption that the RBE for the same cell line and the same biologic endpoint may be assumed to be dependent on LET alone."<sup>31</sup> However, this is the first time a general model of RBE as a function of LET was formulated for all ion beams, and this RBE model could be called the LET power model.

For PIDE data, each set of ion beam irradiation experiments has a corresponding set of photon irradiation, where  $\alpha$ ,  $\beta$ , and the energy of the photon beam are reported. Thus,  $D_{\text{ref}}$  for each SF could be easily calculated. However, it should be emphasized that, in determining  $a$ ,  $b$ ,  $c$ , and  $D_1$  for Equations (5) and (6), photon irradiation was not part of the equation and was only used in Equation (9) for calculating RBE. In other words, Equations (5) and (6) describe the biological effectiveness of ion beams instead of the RBE of ion beams described in previous investigations.

To validate the results, the coefficient of determination ( $R^2$ ) between the RBE determined using Equation (9) and from the measured data was calculated for different ions.

### 3 | RESULTS

Table 1 summarizes all cell irradiation experiments included in PIDE. Based on the reported  $\alpha$  and  $\beta$  dose versus SF or ( $D$ , SF), all experiments were recreated in Figure 1A, where each curve corresponds to one experiment set. Fluence could then be calculated from  $D$  using the reported LET and Equation (1), where the ( $D$ , SF) data could now be rewritten as ( $\Phi$ ,  $L_\infty$ , SF). Thus, the  $\Phi$  and  $L_\infty$  required to achieve a specific SF for each experiment sets could be plotted. Figure 1B shows the  $\Phi$  and  $L_\infty$  required to achieve an SF of 0.8 for all experiments, with experiments reported by Weyrather et al.<sup>32</sup> highlighted. Weyrather et al. studied three cell lines, V79, CHO-K1 and xrs5. As shown in the figure, the results from each of the cell lines form two distinctive lines, above and below 150 keV/ $\mu$ m, and each of them deviates from the dose line, indicating that the dose is not a good predictor for biological response. The separation among the lines for the three cell types and the difference in slopes indicate different parameters,  $D_1$  and  $c$ . Figure 1C shows the  $\Phi$  and  $L_\infty$  required to achieve an SF of 0.5 for different ions and all experiments. Figure 1D shows the  $\Phi$  and  $L_\infty$  required to achieve an SF of 0.1 for different ions and V79 cells in asynchronous cell cycle phases. Figures 1A–C show

all 1118 sets of experiments, whereas Figure 1D shows 278 sets of V79 experiments, as detailed in Table 1.

Table 2 summarizes the linear fitting results for  $a$ ,  $b$ ,  $c$ , and  $D_1$  for the V79 cell line in asynchronous cell cycle phases, as shown in Figure 1D, with proton, carbon, and high LET (>150 keV/ $\mu$ m) irradiation. Table 2 also shows the calculated  $D_{ref}$  using the reported  $\alpha$  and  $\beta$  of photon experiments paired with PIDE ion beam experiments.

Using the linear fitting results of  $c$ ,  $D_1$  and  $D_{ref}$ , RBE for various ion beams at different SF can then be calculated with Equation (9). Figure 2 shows the calculated RBE using the LET power model (Equation 9) compared against the calculated RBE with experimental data (Equation 8) at SF of 0.8, 0.5, and 0.1 for various ions. The coefficient of determination ( $R^2$ ) between RBE determined using the model and the experimental data for different ions at different SF were calculated and are tabulated in Table 3.

### 4 | DISCUSSION

The absorbed dose has been used to relate the imparted radiation energy to biological effects, specifically for in-vitro cell experiments, cell death, and survival fractionations. In the form of the product of fluence and LET, the implicit assumptions of the dose are that the relative contribution from fluence and LET are equal and that spatial distribution of ionization events is not relevant. This study demonstrated overwhelming evidence that while both are important

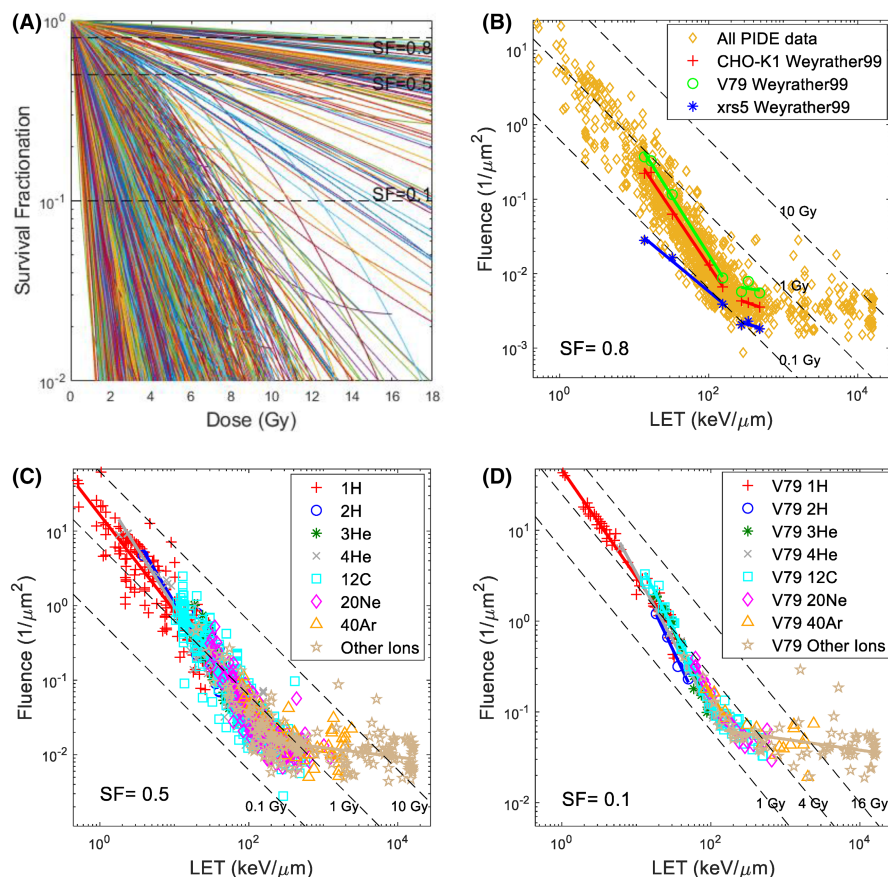
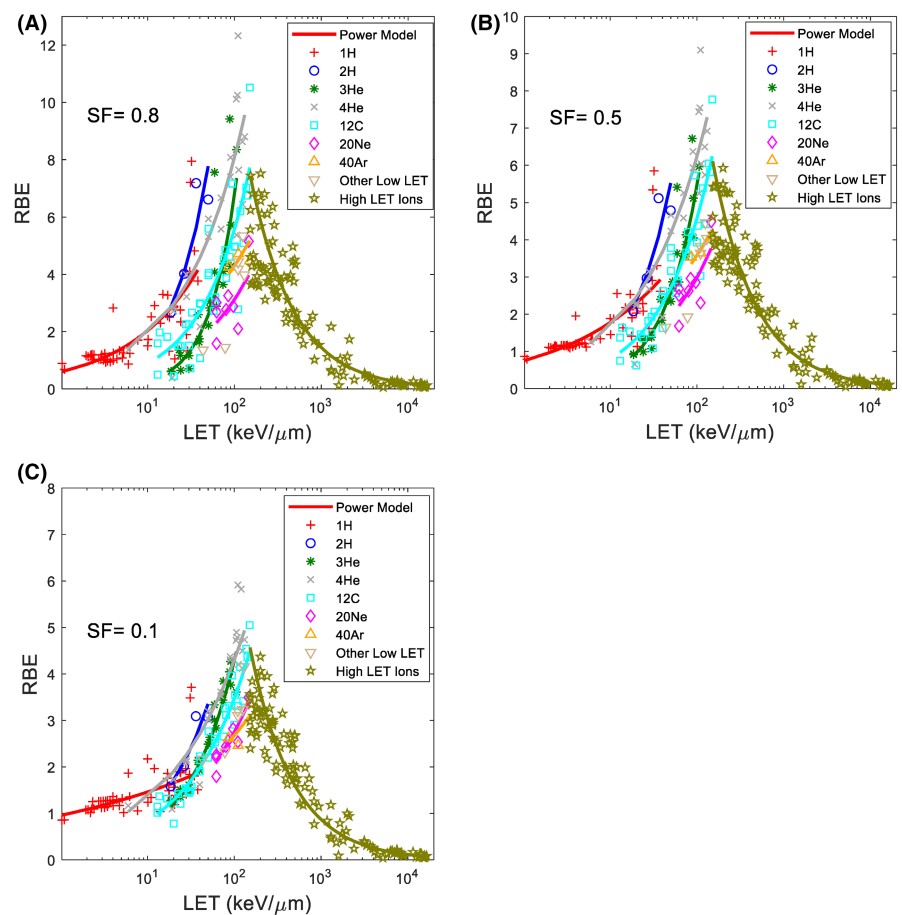


FIGURE 1 LET and Fluence required to achieve a certain SF in different ion beam cell experiments in PIDE. (A) LQ model fitted survival curves for all 1118 sets of experiments. (B) Fluence and LET needed to achieve SF = 0.8, for all ion beam cell irradiation experiments in PIDE, with experiments reported by Weyrather et al.<sup>32</sup> highlighted. (C) Fluence and LET needed to achieve SF = 0.5, for all beam cell irradiation experiments in PIDE. (D) Fluence and LET needed to achieve SF = 0.1, for V79 cell line in asynchronous cell cycle phase, irradiated by different types of ions

**TABLE 2** Parameters  $a$ ,  $b$ ,  $c$ , and  $D_1$  for cell irradiation with 1H, 12C, and high LET ion beam ( $>150\text{ keV}/\mu\text{m}$ ) at SF 0.8, 0.5, and 0.1, of V79 cell line in asynchronous cell phase. Photon dose ( $D_{\text{ref}}$ ) needed to achieve the same SF was also shown

	SF	$a$	$b$	$c$	$D_1$	$D_{\text{ref}}$ (Gy)
1H	0.8	$-0.041 \pm 0.0028$	$2.01 \pm 0.029$	$1.48 \pm 0.11$	$2.54 \pm 0.75$	$1.35 \pm 0.40$
	0.5			$1.33 \pm 0.07$	$4.23 \pm 0.76$	$3.17 \pm 0.62$
	0.1			$1.17 \pm 0.06$	$7.33 \pm 0.99$	$7.20 \pm 1.05$
12C ( $<150\text{ keV}/\mu\text{m}$ )	0.8	$-2.2\text{e-}3 \pm 3.3\text{e-}4$	$2.22 \pm 0.04$	$1.72 \pm 0.14$	$8.04 \pm 5.99$	$1.35 \pm 0.40$
	0.5			$1.60 \pm 0.10$	$13.00 \pm 6.38$	$3.17 \pm 0.62$
	0.1			$1.51 \pm 0.07$	$23.33 \pm 7.73$	$7.20 \pm 1.05$
High LET ion beam ( $>150\text{ keV}/\mu\text{m}$ )	0.8	$-221.9 \pm 2.4$	$1.12 \pm 0.003$	$0.134 \pm 0.04$	$2.0\text{e-}3 \pm 0.7\text{e-}3$	$1.35 \pm 0.40$
	0.5			$0.124 \pm 0.04$	$5.8\text{e-}3 \pm 1.8\text{e-}3$	$3.17 \pm 0.62$
	0.1			$0.111 \pm 0.03$	$1.7\text{e-}2 \pm 4.6\text{e-}3$	$7.20 \pm 1.05$

**FIGURE 2** RBE as a function of LET, for asynchronized V79 cell irradiations with different ions. Solid lines: RBE calculated using LET power model (Equation 9). Data points: RBE calculated using reported experiment results compiled in PIDE, total of 278, detailed in Table 1. Figure (A–C) shows results for SF = 0.8, 0.05, and 0.1, respectively



to cell survival, fluence and LET have different contributions at different LET and fluence ranges. The relative importance of the two is described by a new parameter  $c$ , as shown in Equation (6). As a result, both fluence and LET could be viewed as variables of SF, which is, in essence, a unitless cumulative probability distribution function.

In the LET–fluence–SF plots, as shown in Figures 1B–D, each data point represents the intersection between the specific SF line and the dose–SF curve, as shown in Figure 1A. It is worth pointing out that, according to Equation (2), with varying LET, one would need different fluence to achieve the same dose, and these points also

form an “iso-dose” line on the log–log scale, where each point on the line represents the same dose. Several iso-dose lines were plotted as dotted lines in the figures and intersected with the fluence–LET line, which was described by parameters  $c$  and  $D_1$ , to achieve the specific SF. The observation that the experimental data does not follow an iso-dose line again highlights that the same dose does not correspond to the same response for ion beams with varying LET. Instead, the relationship between fluence and LET follows a line with slope  $c$ , where  $c$  varies for different SF, as shown in Table 2.  $D_1$  represents the intersection point between the fluence–LET line and

TABLE 3 Coefficient of determination ( $R^2$ ) of the power model vs. measurement for V79 cell line in asynchronous cell phase irradiation using varies ion types, as shown in Figure 2

Ion type	Number of experiments	SF		
		0.8	0.5	0.1
$^1\text{H}$	50	0.454	0.437	0.432
$^2\text{H}$	4	0.900	0.923	0.959
$^3\text{He}$	23	0.765	0.823	0.833
$^4\text{H}$	22	0.552	0.768	0.870
$^{12}\text{C}^a$	34	0.755	0.849	0.870
$^{20}\text{Ne}^a$	8	0.770	0.770	0.770
$^{40}\text{Ar}^a$	3	0.612	0.632	0.664
High LET ions	128	0.543	0.727	0.820

<sup>a</sup>LET $\leq$ 150 keV/ $\mu\text{m}$  only.

LET of 1 keV/ $\mu\text{m}$  and numerically equals the dose needed to achieve the specific SF using an ion beam with 1 keV/ $\mu\text{m}$ .

Equations (5) and (6) represent a general formalism of biological effectiveness of ion beams. As shown above, the derivation of the equations and parameters was completely independent from the photons, which separates the current study from previous investigations. Figure 1B shows how the same equations could be applied to different cell types (CHO-K1, V79, and xrs5), only with different parameters  $D_1$  and  $c$ . As shown in Table 2, as LET increase with heavier ions, the biological effectiveness drifts further from photon. For heavier ions, such as carbon ions, there is a LET threshold, above which increasing LET no longer increases the biological effectiveness of the ion beam, or the curves “flatten out.” The same fluence of high LET beams yields similar cell killing.<sup>13</sup> To increase cell killing, one must increase the fluence or increase the number of ions. However, the same Equations (5) and (6) could still be used to describe the biological effectiveness for these high LET ion beams. This fundamental yet critical observation was overlooked in previous investigations of the RBE of ion beams, where assumptions that directly contradict the observation were made in some cases. Once the biological effectiveness of the ion beam was found, it was straightforward to calculate the RBE. As mentioned above, since the relationship between the biological effect of ion beams and beam characteristics were derived independently of the reference irradiation, unlike other RBE models, no additional assumptions were made in the current study. LET versus RBE data similar to Figure 2 has been shown in prior literature,<sup>16,31,33,34</sup> but the current study is the first to derive a generic closed-form expression for all ion beams. The coefficient of determination ( $R^2$ ) of RBE determined using the model and experimental data is calculated and tabulated in Table 3 for various ions and SF. The relatively low  $R^2$  values of the proton data are due to the high uncertainty in the experimental dataset, as previously explored, and had in part justified the use of a constant RBE value of 1.1.<sup>35</sup> To further validate the model in the proton domain, high quality experimental data with precise LET and fluence data would be necessary.

Other factors, such as the oxygen level (the oxygen enhancement ratio)<sup>36</sup> and the cell cycle<sup>37</sup> also have significant impacts on the biological endpoints and have also been studied extensively. The same method could be expanded and applied to these investigations but is outside the scope of the current study. Uncertainties are inherently large with cell experiments because of the complexity of such investigations and the statistical nature of cell killing. For example, it is impossible to directly measure the dose required to achieve a specific SF for a particular cell line and ion beam, as SF could only be measured days after the cell irradiation. Thus, such data could only be acquired through modeling and interpolation of raw data. Nevertheless, comparable confidence intervals for  $D_1$  and  $D_{\text{ref}}$  for various SF, between proton and photon irradiation, were shown in Table 2, noting that both photon and proton beams could be in the 1 keV/ $\mu\text{m}$  range. In contrast, for heavier ions, the LET ranges move further away from photons as the atomic number increases (there were no 1 keV/ $\mu\text{m}$  beams for heavier ions), thus making the direct comparison with photons more challenging. Another notable source of uncertainty arises from the reported LET. Different variants of LET, including dose averaged LET, track averaged LET, in addition to LET $_{\infty}$ , were reported in the literature, which could also lead to uncertainties in the determination of fluence using Equation (2). The rationale for using different LET variations is outside the scope of the current study and will not be further discussed.

Cell survival fractionation could be written as a function of fluence and LET for all ion beam irradiations. The close form relationship could be used for proton and ion beam radiotherapy applications.

## ACKNOWLEDGMENTS

I acknowledge the PIDE project for compiling available ion beam in-vitro cell irradiation data.

## CONFLICT OF INTEREST

Author declares no competing interests.

## DATA AVAILABILITY STATEMENT

All data are available through PIDE. [https://www.gsi.de/work/forschung/biophysik/forschungsfelder/radiobiological\\_modelling/pide\\_project](https://www.gsi.de/work/forschung/biophysik/forschungsfelder/radiobiological_modelling/pide_project)

## ORCID

Heng Li  <https://orcid.org/0000-0003-4815-0537>

## REFERENCES

- Desouky O, Ding N, Zhou G. Targeted and non-targeted effects of ionizing radiation. *J Radiat Res Appl Sci*. 2015;8:247-254.
- Olive PL. The role of DNA single- and double-strand breaks in cell killing by ionizing radiation. *Radiat Res*. 1998;150:S42-S51.
- Sinclair WK. Cyclic X-ray responses in mammalian cells in vitro. *Radiat Res*. 1968;33:620-643.
- Todd P. Heavy-ion irradiation of cultured human cells. *Radiat Res Suppl*. 1967;7:196-207.



5. Till JE, McCulloch EA. A direct measurement of the radiation sensitivity of normal mouse bone marrow cells. *Radiat Res.* 1961;14:213-222.
6. Hewitt HB, Wilson CW. Survival curves for tumor cells irradiated in vivo. *Ann N Y Acad Sci.* 1961;95:818-827.
7. Suzuki M, Kase Y, Yamaguchi H, Kanai T, Ando K. Relative biological effectiveness for cell-killing effect on various human cell lines irradiated with heavy-ion medical accelerator in Chiba (HIMAC) carbon-ion beams. *Int J Radiat Oncol Biol Phys Ther.* 2000;48:241-250.
8. McMahon SJ. The linear quadratic model: usage, interpretation and challenges. *Physics in Medicine & Biology.* 2018;64:01TR01.
9. Durante M, Loeffler JS. Charged particles in radiation oncology. *Nat Rev Clin Oncol.* 2021;7:37-43.
10. Franken NA, Rodermond HM, Stap J, Haveman J, Van Bree C. Clonogenic assay of cells in vitro. *Nat Protoc.* 2006;1:2315-2319.
11. Blakely EA, Tobias CA, Yang TC, Smith KC, Lyman JT. Inactivation of human kidney cells by high-energy monoenergetic heavy-ion beams. *Radiat Res.* 1979;80:122-160.
12. Zhang S, Wimmer-Schweingruber RF, Yu J, et al. First measurements of the radiation dose on the lunar surface. *Sci Adv.* 2020;6:eaaz1334.
13. Barendsen G. Relative effectiveness of ionizing radiations in relation to let and the influence of oxygen. *Biophysical Aspects of Radiation Quality IAEA, 1966;* 44-57.
14. Brooks AL. Chromosome damage in liver cells from low dose rate alpha, beta, and gamma irradiation: derivation of RBE. *Science.* 1975;190:1090-1092.
15. Failla G, Henshaw P. The relative biological effectiveness of X-rays and gamma rays. *Radiology.* 1931;17:1-43.
16. Friedrich T, Scholz U, Elsässer T, Durante M, Scholz M. Systematic analysis of RBE and related quantities using a database of cell survival experiments with ion beam irradiation. *J Radiat Res.* 2013;54:494-514.
17. Units ICoR. Report of the International Commission on Radiological Units and Measurements (ICRU), 1959. US Department of Commerce, National Bureau of Standards, 1961
18. ICRU. Linear Energy Transfer, ICRU Report No. 16. International Commission on Radiation Units Measurements. 1970.
19. Scholz M, Kraft G. Calculation of heavy ion inactivation probabilities based on track structure, X ray sensitivity and target size. *Radiat Prot Dosimetry.* 1994;52:29-33.
20. Scholz M, Kraft G. Track structure and the calculation of biological effects of heavy charged particles. *Adv Space Res.* 1996;18:5-14.
21. Scholz M, Kellerer A, Kraft-Weyrather W, Kraft G. Computation of cell survival in heavy ion beams for therapy. *Radiat Environ Biophys.* 1997;36:59-66.
22. Grün R, Friedrich T, Elsässer T, et al. Impact of enhancements in the local effect model (LEM) on the predicted RBE-weighted target dose distribution in carbon ion therapy. *Phys Med Biol.* 2012;57:7261-7274.
23. Inaniwa T, Furukawa T, Kase Y, et al. Treatment planning for a scanned carbon beam with a modified microdosimetric kinetic model. *Phys Med Biol.* 2010;55:6721-6737.
24. Hawkins RB. A statistical theory of cell killing by radiation of varying linear energy transfer. *Radiat Res.* 1994;140:366-374.
25. Hawkins RB. A microdosimetric-kinetic model for the effect of non-Poisson distribution of lethal lesions on the variation of RBE with LET. *Radiat Res.* 2003;160:61-69.
26. Kamp F, Cabal G, Mairani A, Parodi K, Wilkens JJ, Carlson DJ. Fast biological modeling for voxel-based heavy ion treatment planning using the mechanistic repair-misrepair-fixation model and nuclear fragment spectra. *Int J Radiat Oncol Biol Phys Ther.* 2015;93:557-568.
27. Mairani A, Dokić I, Magro G, et al. Biologically optimized helium ion plans: calculation approach and its in vitro validation. *Phys Med Biol.* 2016;61:4283-4299.
28. Scholz M, Kraft G. The physical and radiobiological basis of the local effect model: a response to the commentary by R. Katz. *Radiation Res.* 2004;161:612-620.
29. Stewart RD, Carlson DJ, Butkus MP, Hawkins R, Friedrich T, Scholz M. A comparison of mechanism-inspired models for particle relative biological effectiveness (RBE). *Med Phys.* 2018;45:e925-e952.
30. Choi J, Kang JO. Basics of particle therapy II: relative biological effectiveness. *Radiat Oncol J.* 2012;30:1-13.
31. Sorensen BS, Overgaard J, Bassler N. In vitro RBE-LET dependence for multiple particle types. *Acta Oncol.* 2011;50:757-762.
32. Weyrather WK, Ritter S, Scholz M, Kraft G. RBE for carbon track-segment irradiation in cell lines of differing repair capacity. *Int J Radiat Biol.* 1999;75:1357-1364.
33. Cunha M, Monini C, Testa E, Beuve M. NanOx, a new model to predict cell survival in the context of particle therapy. *Phys Med Biol.* 2017;62:1248-1268.
34. Parisi A, Sato T, Matsuya Y, et al. Development of a new microdosimetric biological weighting function for the RBE10 assessment in case of the V79 cell line exposed to ions from 1H to 238U. *Phys Med Biol.* 2020;65:235010.
35. Paganetti H. Significance and implementation of RBE variations in proton beam therapy. *Technol Cancer Res Treat.* 2003;2:413-426.
36. Wenzl T, Wilkens JJ. Modelling of the oxygen enhancement ratio for ion beam radiation therapy. *Phys Med Biol.* 2011;56:3251-3268.
37. Mitchell J, Bedford J, Bailey S. Dose-rate effects on the cell cycle and survival of S3 HeLa and V79 cells. *Radiat Res.* 1979;79:520-536.

#### SUPPORTING INFORMATION

Additional supporting information may be found in the online version of the article at the publisher's website.

**How to cite this article:** Li H. Biological effectiveness and relative biological effectiveness of ion beams for in-vitro cell irradiation. *Cancer Sci.* 2022;113:2807-2813. doi: [10.1111/cas.15446](https://doi.org/10.1111/cas.15446)